

Methane Clathrate Hydrates Formed within Hydrophilic and Hydrophobic Media: Kinetics of Dissociation and Distortion of Host Structure

Satoshi Takeya,^{*,†} Hiroshi Fujihisa,[†] Yoshito Gotoh,[†] Vladimir Istomin,[‡] Evgeny Chuvilin,[§] Hirotoshi Sakagami,^{||} and Akihiro Hachikubo^{||}

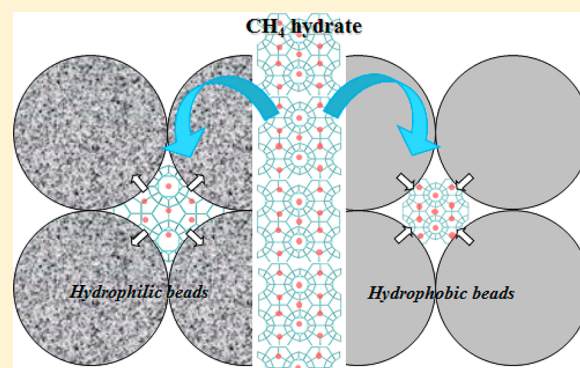
[†]National Institute of Advanced Industrial Science and Technology (AIST), Tsukuba 305-8565, Japan

[‡]Gazprom VNIIGAZ LLC, Moscow Region, 142717, Russia

[§]Moscow State University, Moscow 119991, Russia

^{||}Kitami Institute of Technology, 165 Koen-cho, Kitami 090-8507, Japan

ABSTRACT: The crystal structure and dissociation processes of methane (CH₄) hydrates were investigated to better understand their stability in a natural environment. By using powder X-ray diffraction, we found that the unit-cell parameters of the hydrates formed with fine hydrophilic and hydrophobic beads were respectively larger and smaller by 0.02 Å than the unit-cell parameters of simple CH₄ hydrates. In addition, it was found that CH₄ hydrates formed with hydrophobic beads dissociated quickly above 200 K, whereas the CH₄ hydrates formed with hydrophilic beads are stable up to about 273 K (Hachikubo et al. *Phys. Chem. Chem. Phys.* **2011**, *13*, 17449–17452). The interfacial forces inside the intergranular pores or void spaces of the beads affect the kinetics of dissociation of CH₄ hydrate and are important for both the macroscopic and the crystallographic structures.



INTRODUCTION

Gas hydrates are crystalline host–guest compounds where guest molecules are inside hydrogen-bonded water cages. Natural gas hydrates, which contain methane (CH₄) as a major component, exist under conditions of low temperatures and high partial pressures of the guest gases. Because natural gas hydrates exist in sea and lake bottom sediments and permafrost layers, they are considered to be a possible source of energy.^{1–3} A comprehensive understanding of the stability of these hydrates is also important for their potential effects on global climate change when they dissociate.^{4–7} There have been many studies on the dissociation mechanisms of gas hydrates in the absence of sediments or porous materials; these studies are motivated by physicochemical perspectives or from gas storage applications.^{8–22} Although many studies have been done concerning the thermodynamic stability of gas hydrates within pore spaces,^{23–27} much less is known about their physical properties under natural conditions and their dissociation mechanisms at the microscopic level,^{28–30} except for recent simulations.^{31–33}

Recently, we have found that the CH₄ hydrates formed with hydrophilic glass beads that are less than a few micrometers in size remained stable up to about the melting point of ice (273 K), even though this temperature is well outside the zone of the hydrate thermodynamic stability.³⁴ This suggests that CH₄ hydrates occurring naturally within the pores of fine particles

at low temperatures, such as clays, would be stable even though their thermodynamic stability within mesopores (less than 10 nm) is lower than that of bulk CH₄ hydrates because of the Gibbs–Thomson effect. In this respect, the effects of interfacial forces inside confined spaces may affect the stability of CH₄ hydrates.

To better understand the effect by interfacial force within a confined space to CH₄ hydrate, we report here the crystallographic structures of CH₄ hydrates within intergranular pores, that is, voids, formed by hydrophobic and hydrophilic beads. Powder X-ray diffraction (PXRD) and Raman spectroscopy were employed to characterize the crystal structures of CH₄ hydrates and their cage occupancies in several types of beads, which have sizes corresponding to the macropore scale (>50 nm). Also, temperature-dependent PXRD measurements were performed to characterize the dissociation processes of CH₄ hydrates within the void spaces.

EXPERIMENTAL METHODS

CH₄ hydrates were formed from mixtures of water and similarly sized and hydrophobic³⁴ or hydrophilic nonporous beads with a smooth surface (see Figure 1). Details of all the beads are

Received: December 13, 2012

Revised: March 8, 2013

Published: March 8, 2013

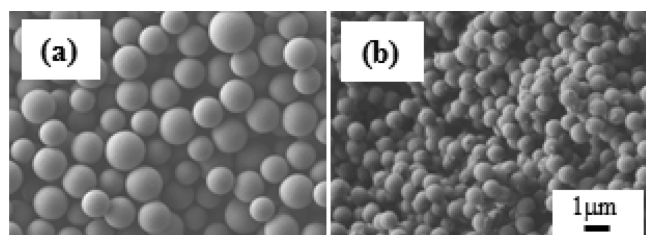


Figure 1. Field-effect scanning electron microscope images of hydrophobic beads (JEOL Ltd. model JSM-7400F): (a) TP-120 and (b) MSP-N050.

summarized in Table 1. About 1 g of fine ice-powder (<0.05 mm mean grain size) was mixed with 5 g of beads in a 20 mL high-pressure cell at 255 K. The cell was evacuated and kept at 274 K for several hours to obtain uniform distribution of water in the void of the sample. Then, it was pressurized up to 5 MPa with research-grade CH₄ (99.99% purity, Takachiho Chemical Industry, Tokyo, Japan) for more than 36 h to form CH₄ hydrates. After no significant pressure decreases (less than 0.01 MPa h⁻¹) were observed, the hydrate sample was retrieved from the cell at a temperature below 100 K and under a dry nitrogen-gas atmosphere. Here, the ice-powder mixed with these beads likely to be transformed into CH₄ hydrate inside the void spaces without agglomerations because any apparent CH₄ hydrate particles were not observed after the synthesis process.

PXRD measurements were performed in a 2 θ/θ step scan mode using Cu K α radiation ($\lambda = 1.541 \text{ \AA}$) and parallel beam optics (40 kV, 40 mA; Rigaku model Ultima III). LaB₆ (NIST) was used as an external standard for the 2 θ angle offset. Analysis of unit-cell parameters was performed by a whole-pattern fitting method in the 2 θ range 6–50° using the Rietveld program RIETAN-FP.³⁵ To observe CH₄ hydrate dissociation, samples were mounted under a nitrogen-gas atmosphere and kept below 100 K on a copper PXRD sample holder. Here, sample was filled within the groove of 0.50 mm in depth of the sample holder for achieving fast thermal response caused by temperature ramping for kinetic observation. PXRD measurements were performed over the temperature range 123–273 at 10 K intervals under isothermal temperature conditions for a total scan time of 5 min, and the next scan was started after a heating-up period of about 0.5 min. The measurements over 123–173 K were performed in a vacuum, and those over 173–273 K were performed under a dry nitrogen gas to prevent condensation of water vapor on the sample surface. To analyze

relative occupancies of hydrate cages, Raman spectra of the hydrate samples were obtained at 123 K using a Raman spectrometer (RMP-210; JASCO Corporation) equipped with a 100 mW, 532 nm excitation source, and a single 1800 grooves mm⁻¹ holographic diffraction grating. The spectra were collected with approximately 1.2 cm⁻¹ resolution in the range 2500–3000 cm⁻¹ for CH₄ C–H stretching bands. The spectra were fitted using a Voigt function to obtain the integrated intensities of the two peaks corresponding to CH₄ molecules encaged in large and small cages.

RESULTS AND DISCUSSION

Figure 2 shows PXRD patterns of CH₄ hydrate samples formed with different types of beads. As expected, the samples were

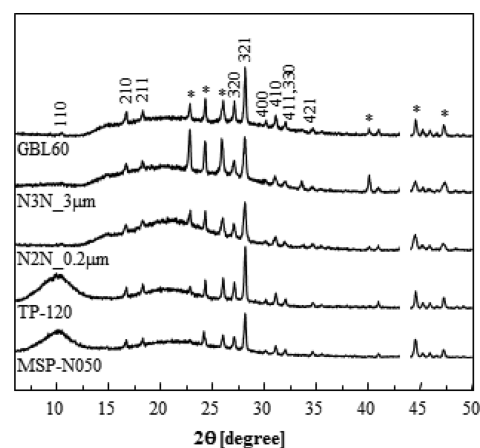


Figure 2. PXRD profiles of CH₄ hydrates formed within different beads. The Miller index of each diffraction peak from the sI hydrate is indicated, and asterisks (*) indicate the diffraction peaks from hexagonal ice. Here, the diffraction peak from Cu of the sample holder at around 43° is excluded.

normal structure I (sI; space group: *Pm3n*) hydrates and include some hexagonal ice (Ih) due to unreacted water. Figure 3 shows the temperature dependence of the unit-cell parameters for the hydrates formed with both hydrophobic and hydrophilic beads. In the temperature range 93–193 K, the unit-cell parameters of the hydrates formed with $\geq 30 \mu\text{m}$ diameter hydrophilic beads are equivalent to those for bulk CH₄ hydrates. However, the unit-cell parameters of the hydrates formed with $\leq 10 \mu\text{m}$ diameter hydrophilic beads are 0.02 Å larger than those for bulk CH₄ hydrates. In contrast, the

Table 1. Characteristics of Beads and Water Content of Samples^a

size of particles, μm	type of beads (company)	material	surface property	specific surface area, $\text{m}^2 \text{g}^{-1}$	water content, %
56.33(7)	GBL-60 (The Association of Powder Process Industry and Engineering)	CaO–Al ₂ O ₃ –SiO ₂ glass	hydrophilic	0.2	14.1
30.82(5)	GBL-30 (The Association of Powder Process Industry and Engineering)	CaO–Al ₂ O ₃ –SiO ₂ glass	hydrophilic	0.4	16.1
8.66(5)	N3N_10 μm (UBE-NITTO KASEI Co., Ltd.)	SiO ₂ glass (99.9%)	hydrophilic	0.3	18.6
3.15(5)	N3N_3 μm (UBE-NITTO KASEI Co., Ltd.)	SiO ₂ glass (99.9%)	hydrophilic	0.7	21.0
0.98(7)	N3N_1 μm (UBE-NITTO KASEI Co., Ltd.)	SiO ₂ glass (99.9%)	hydrophilic	3	17.6
0.11(10)	N2N_0.2 μm (UBE-NITTO KASEI Co., Ltd.)	SiO ₂ glass (99.9%)	hydrophilic	14	20.3
2.0*	TP-120 (MOMENTIVE performance materials)	silicone	hydrophobic	30	18.7
0.6*	MSP-N050 (Nikko Rika Co.)	silicone	hydrophobic	20	18.8

^aThe grain-size distributions were measured using a laser diffraction particle-size analyzer (SALD-2100, Shimadzu Corporation, Kyoto, Japan). Sizes and specific surface area of the hydrophobic beads are those reported by the manufacturers.

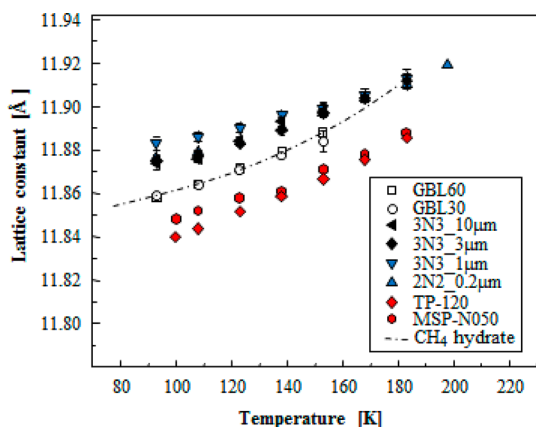


Figure 3. Temperature-dependent CH_4 hydrate unit-cell parameters within various beads. For comparison, the dashed curve is the fit to reported data for bulk CH_4 hydrate.⁴⁵

unit-cell parameters of the CH_4 hydrates formed with hydrophobic beads are 0.02 \AA smaller than those of pure bulk CH_4 hydrates in the same temperature range. The analytical error in the unit-cell parameters is $<0.001 \text{ \AA}$.

The unit-cell size of gas hydrates depends on the type of guest molecule and cage occupancy under isothermal conditions. Figure 4 displays Raman spectra of CH_4 hydrates

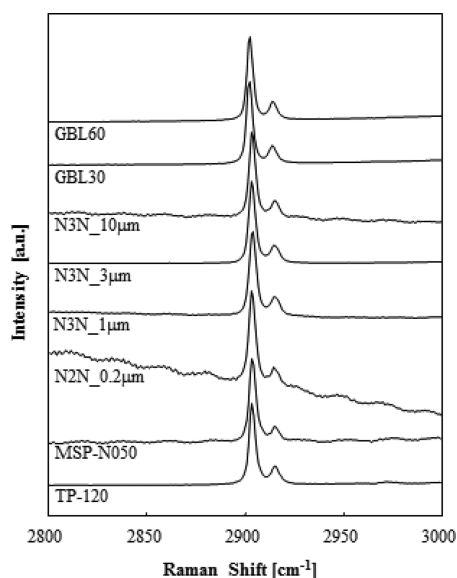


Figure 4. Raman spectra of the C–H symmetric stretch region of the CH_4 hydrates formed within various beads.

formed within voids. The spectra are very similar to those of bulk CH_4 hydrates (not shown), regardless of the bead size and surface properties. The C–H stretch band splitting indicates that the CH_4 partitions between the small (S^{12}) and large ($S^{12}6^2$) cavities of sI, where the lower energy band is assigned to CH_4 in the large cavity and the higher energy band is assigned to CH_4 in the small cavity. The partitioning is small/large = 1:3. This spectroscopic evidence suggests that the cage occupancies of these CH_4 hydrates are almost the same as those observed for bulk CH_4 hydrate, which is consistent with earlier studies of CH_4 hydrates formed in voids ranging 1–100 nm.³⁴ Thus, the differences in the CH_4 hydrate unit-cell sizes are not caused by cage occupancy.

We performed density functional theory calculations using the Castep program to estimate the differences in unit-cell parameters of CH_4 hydrates with those obtained from the hydrophilic beads. The results indicate a variance of 0.016 \AA between the two unit-cell parameters, which corresponds to a pressure difference of 40 MPa. The latter is the same order of magnitude as that estimated from the CH_4 hydrate bulk modulus in high-pressure experiments.³⁶ Thus, the difference in the unit-cell sizes can be caused by the interfacial forces within the void spaces. Here, it should be noted that, at higher temperatures, the unit-cell sizes of the CH_4 hydrates within hydrophilic beads approached those for bulk CH_4 hydrates. This might suggest that liquid water forms between the hydrophilic beads and the hydrate because of dissociation and the rupture of hydrogen bonding between the hydrate and the surface silanol group of silica. In contrast, in the case of CH_4 hydrates within hydrophobic beads, it is not known why the unit-cell sizes of CH_4 hydrate within hydrophobic beads did not also become similar to those for bulk CH_4 hydrates, even at the dissociation temperature (see Figure 3). Because liquid water also forms because of dissociation, this suggests that the differences in the unit-cell sizes are not caused by the liquid within the void spaces.

In earlier studies, natural gas hydrates drilled from the Nankai Trough of Japan probably show a similar trend of unit-cell parameters that depend on sand grain sizes.³⁷ Likewise, the unit-cell parameters of intercalated CH_4 hydrates formed in clay expand with an expansion value comparable to the hydrates caged within hydrophilic beads.³⁸ In addition, liquid water transforms into cubic ice (Ic), but not ice Ih, within hydrophilic mesoporous silica as a function of pore size in the 10 nm range.^{39,40} In contrast, it has been reported that ice Ih is formed in hydrophobic-activated carbon instead of ice Ic.⁴¹ According to these experimental results in this study and reported, we concluded that the host structure of the CH_4 hydrates is affected by the interfacial forces within voids or macropores.

Dissociation of CH_4 hydrates that were formed with the different beads was investigated by temperature-dependent PXRD to characterize void size effects. For the PXRD, each hydrate sample within the beads was finely ground and powdered ($\sim 10 \mu\text{m}$ particle size) to exclude the possibility that the morphology of the CH_4 hydrate is affected by the growth rate⁴² or the type of beads used.⁴³ In our previous study,³⁴ it was shown that hydrate samples coexisting with hydrophilic glass beads $<3 \mu\text{m}$ were preserved up to about 273 K. Figure 5 shows the relative volume ratios for various hydrates as a function of temperature. Almost half the hydrate samples coexisting with both hydrophobic and hydrophilic beads ($<3 \mu\text{m}$) were stable at 200 K; even that temperature is higher than its phase equilibrium temperature. However, the CH_4 hydrates within hydrophobic beads dissociated quickly above 200 K.

The effects of particle size on bulk CH_4 hydrate dissociation have been reported.¹⁴ In the temperature-ramping method, the dissociation rates of large hydrate particles are lower than those of smaller particles. It is therefore expected, according to the particle-size effect, that CH_4 hydrates formed in the small voids of fine beads dissociate readily. CH_4 hydrates within the smaller voids of $<3 \mu\text{m}$ hydrophilic beads were stable up to about 273 K, whereas those in hydrophobic beads completely dissociated below 230 K. These results indicate that CH_4 hydrate stability was affected by surface interactions inside the void space.

With hydrophilic beads, liquid water molecules between the dissociating CH_4 hydrate and the beads work to stabilize the

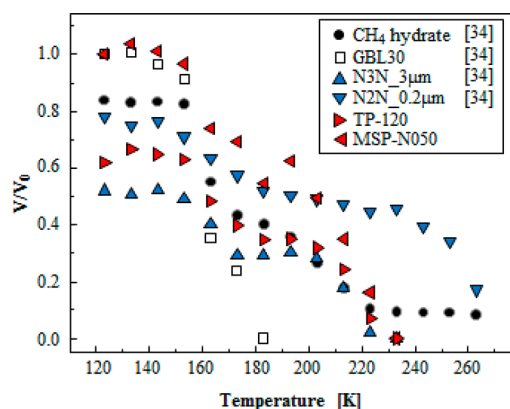


Figure 5. Temperature-dependent volume ratios of CH₄ hydrates for various samples, obtained with PXRD. Initial volume ratios of the CH₄ hydrates were analyzed by the Rietveld method. Other relative volume ratios were analyzed using the reflection for the si(321) crystal plane at $2\theta = 28^\circ$ because the integrated intensity of the X-ray diffraction profile is proportional to the crystal volume.

CH₄ hydrate within the voids. This interpretation is consistent with a recent molecular dynamics simulation,³² which suggests that a water layer between the hydrate phase and the silica surface stabilizes the hydrate phase relative to the case where the hydrate is in direct contact with the silica. In contrast, liquid water cannot seal the void space within hydrophobic beads. Therefore, it is expected that the CH₄ hydrates within the small void spaces of hydrophobic beads are likely to dissociate.

Although further quantitative experimental work is still needed to understand the correlation between the unit-cell size and the stability of CH₄ hydrates within void, macro, or smaller pores, the results reported here suggest that CH₄ hydrate stability is strongly affected by the surrounding. These results suggest that, in the event of an assessment of natural gas hydrates under natural settings, properties of the potential sediments should be considered. From an applications viewpoint, porous materials or beads can be used for hydrate formation and dissociation reactors because they provide sufficient contact time and volume between the gas and water contained within the void or pores.⁴⁴ Another practical application is that the dissociation kinetics of CH₄ hydrates can be controlled by using different materials.

SUMMARY

With PXRD and Raman spectroscopy, we characterized the crystal structure of CH₄ hydrates formed within different types (hydrophobic vs hydrophilic) and sizes of beads. We found that the unit-cell parameters of the hydrates formed within <10 µm hydrophilic beads were 0.02 Å larger than those for bulk CH₄ hydrates over the temperature range 90–200 K. In contrast, the unit-cell parameters of the CH₄ hydrates within hydrophobic beads were 0.02–0.04 Å smaller than those of pure CH₄ hydrates. We also found that the cage occupancies of these hydrates were almost the same as bulk CH₄ hydrate. These results are consistent with those previously reported for CH₄ hydrates coexisting with soil or clay. Thus, we concluded that the host structure of the CH₄ hydrates is affected by the interfacial forces within voids.

The dissociation of CH₄ hydrates formed within the voids of different beads was investigated by temperature-dependent PXRD. The CH₄ hydrates formed within fine hydrophobic beads dissociated quickly above 200 K and were unstable above

230 K. However, CH₄ hydrates within fine hydrophilic beads were stable up to 273 K. The CH₄ hydrate stability was clearly dependent on surface interactions inside the void spaces. Accordingly, we conclude that the effects of interfacial forces inside the void (intergranular pores) space, being formed by submicrometer-sized beads, are critical to the understanding of CH₄ hydrate stability.

AUTHOR INFORMATION

Corresponding Author

*Phone: 81-29-861-4506; fax: 81-29-861-4845; e-mail: s.takeya@aist.go.jp.

Notes

The authors declare no competing financial interest.

ACKNOWLEDGMENTS

Part of this research was supported by the Japan Society for the Promotion of Science (JSPS) and the Russian Foundation for Basic Research (RFBR) under the Japan–Russia Research Cooperative Program. This research was also supported by the Japan Society for the Promotion of Science KAKENHI 22540485.

REFERENCES

- (1) Sloan, E. D. Fundamental Principles and Applications of Natural Gas Hydrates. *Nature* **2003**, *426*, 353–363.
- (2) Makogon, Y. F.; Holditch, S. A.; Makogon, T. Y. Natural Gas-Hydrates — A Potential Energy Source for the 21st Century. *J. Pet. Sci. Eng.* **2007**, *56*, 14–31.
- (3) Boswell, R.; Collett, T. S. Current Perspectives on Gas Hydrate Resources. *Energy Environ. Sci.* **2011**, *4*, 1206–1215.
- (4) Sloan, L. C.; Walker, J. C. G.; Moore, T. C.; Rea, D. K.; Zachos, J. C. Possible Methane-Induced Polar Warming in the Early Eocene. *Nature* **1992**, *357*, 320–322.
- (5) Sluijs, A.; Brinkhuis, H.; Schouten, S.; Bohaty, S. M.; John, C. M.; Zachos, J. C.; Reichert, G. J.; Sinninghe, J. S.; Damsté, E.; Crouch, M.; Dickens, G. R. Environmental Precursors to Rapid Light Carbon Injection at the Palaeocene/Eocene Boundary. *Nature* **2007**, *450*, 1218–1221.
- (6) Kennedy, M.; Mrofka, D.; von der Borch, C. Snowball Earth Termination by Destabilization of Equatorial Permafrost Methane Clathrate. *Nature* **2008**, *453*, 642–645.
- (7) Guillemette, M.; Edouard, B. Geochemical Evidence for a Large Methane Release during the Last Deglaciation from Marmara Sea Sediments. *Geochim. Cosmochim. Acta* **2010**, *74*, 1537–1550.
- (8) Stern, L. A.; Circone, S.; Kirby, S. H.; Durham, W. B. Anomalous Preservation of Pure Methane Hydrate at 1 atm. *J. Phys. Chem. B* **2001**, *105*, 1756–1762.
- (9) Takeya, S.; Shimada, W.; Kamata, Y.; Ebinuma, T.; Uchida, T.; Nagao, J.; Narita, H. In Situ X-ray Diffraction Measurements of the Self-Preservation Effect of CH₄ Hydrate. *J. Phys. Chem. A* **2001**, *105*, 9756–9759.
- (10) Komai, T.; Kang, S. P.; Yoon, J. H.; Yamamoto, Y.; Kawamura, T.; Ohtake, M. In Situ Raman Spectroscopy Investigation of the Dissociation of Methane Hydrate at Temperatures Just below the Ice Point. *J. Phys. Chem. B* **2004**, *108*, 8062–8068.
- (11) Kuhs, W. F.; Genov, G.; Staykova, D. K.; Hansen, T. Ice Perfection and Onset of Anomalous Preservation of Gas Hydrates. *Phys. Chem. Chem. Phys.* **2004**, *6*, 4917–4920.
- (12) Shimada, W.; Takeya, S.; Kamata, Y.; Uchida, T.; Nagao, J.; Ebinuma, T.; Narita, H. Texture Change of Ice on Anomalous Preserved Methane Clathrate Hydrate. *J. Phys. Chem. B* **2005**, *109*, 5802–5807.
- (13) Takeya, K.; Nango, K.; Sugahara, T.; Ohgaki, K.; Tani, A. Activation Energy of Methyl Radical Decay in Methane Hydrate. *J. Phys. Chem. B* **2005**, *109*, 21086–21088.

- (14) Takeya, S.; Uchida, T.; Nagao, J.; Ohmura, R.; Shimada, W.; Kamata, Y.; Ebinuma, T.; Narita, H. Particle Size Effect of CH₄ Hydrate for Self-Preservation. *Chem. Eng. Sci.* **2005**, *60*, 1383–1387.
- (15) Istomin, V. A.; Yakushev, V. S.; Makhonina, N. A.; Kwon, V. G.; Chuvilin, E. M. Self-Preservation Phenomenon of Gas Hydrates. *Gas Ind. Russ.* **2006**, *4*, 16–27.
- (16) Takeya, S.; Ripmeester, J. A. Dissociation Behavior of Clathrate Hydrates to Ice and Dependence on Guest Molecules. *Angew. Chem., Int. Ed.* **2008**, *47*, 1276–1279.
- (17) Melnikov, V. P.; Nesterov, A. N.; Reshetnikov, A. M.; Zavodovsky, A. G. Evidence of Liquid Water Formation during Methane Hydrates Dissociation below the Ice Point. *Chem. Eng. Sci.* **2009**, *64*, 1160–1166.
- (18) Falenty, A.; Kuhs, W. F. “Self-Preservation” of CO₂ Gas Hydrates—Surface Microstructure and Ice Perfection. *J. Phys. Chem. B* **2009**, *113*, 15975–15988.
- (19) Takeya, S.; Ripmeester, J. A. Anomalous Preservation of CH₄ Hydrate and Its Dependence on the Morphology of Hexagonal Ice. *ChemPhysChem* **2010**, *11*, 70–73.
- (20) Melnikov, V. P.; Nesterov, A. N.; Reshetnikov, A. M.; Istomin, V. A.; Kwon, V. G. Stability and Growth of Gas Hydrates below the Ice–Hydrate–Gas Equilibrium Line on the P–T Phase Diagram. *Chem. Eng. Sci.* **2010**, *65*, 906–914.
- (21) Ohno, H.; Nishimura, O.; Suzuki, K.; Narita, H.; Nagao, J. Morphological and Compositional Characterization of Self-Preserved Gas Hydrates by Low-Vacuum Scanning Electron Microscopy. *PhysChemPhys* **2011**, *12*, 1661–1665.
- (22) Takeya, S.; Yoneyama, A.; Ueda, K.; Hyodo, K.; Takeda, T.; Mimachi, H.; Takahashi, M.; Iwasaki, T.; Sano, K.; Yamawaki, H.; Gotoh, Y. Nondestructive Imaging of Anomally Preserved Methane Clathrate Hydrate by Phase Contrast X-ray Imaging. *J. Phys. Chem. C* **2011**, *115*, 16193–16199.
- (23) Handa, Y. P.; Stupin, D. Thermodynamic Properties and Dissociation Characteristics of Methane and Propane Hydrates in 70-Å-Radius Silica Gel Pores. *J. Phys. Chem.* **1992**, *96*, 8599–8603.
- (24) Uchida, T.; Ebinuma, T.; Ishizaki, T. Dissociation Condition Measurements of Methane Hydrate in Confined Small Pores of Porous Glass. *J. Phys. Chem. B* **1999**, *103*, 3659–3662.
- (25) Seo, Y.; Lee, H.; Uchida, T. Methane and Carbon Dioxide Hydrate Phase Behavior in Small Porous Silica Gels: Three-Phase Equilibrium Determination and Thermodynamic Modeling. *Langmuir* **2002**, *18*, 9164–9170.
- (26) Anderson, R.; Llamedo, M.; Tohidi, B.; Burgass, R. W. Experimental Measurement of Methane and Carbon Dioxide Clathrate Hydrate Equilibria in Mesoporous Silica. *J. Phys. Chem. B* **2003**, *107*, 3507–3514.
- (27) Kang, S. P.; Lee, J. W.; Ryu, H. J. Phase Behavior of Methane and Carbon Dioxide Hydrates in Meso- and Macro-Sized Porous Media. *Fluid Phase Equilib.* **2008**, *274*, 68–72.
- (28) Ershov, E. D.; Yakushev, V. S. Experimental Research on Gas Hydrate Decomposition in Frozen Rocks. *Cold Reg. Sci. Technol.* **1992**, *20*, 147–156.
- (29) Chuvilin, E. M.; Guryeva, O. M. Experimental Study of Self-Preservation Effect of Gas Hydrates in Frozen Sediments. *Proceedings of the 9th International Conference on Permafrost*, Fairbanks, AK, June 29–July 3, 2008; Vol. 1, pp 263–267.
- (30) Chuvilin, E. M.; Kozlova, E. V. Experimental Estimation of Hydrate-Containing Sediments Stability. *Proceedings of the 5th International Conference on Gas Hydrate*, Trondheim, Norway, June 13–16, 2005; Vol. 5, pp 1540–1547.
- (31) Liang, S.; Rozmanov, D.; Kusalik, P. G. Crystal Growth Simulations of Methane Hydrates in the Presence of Silica Surfaces. *Phys. Chem. Chem. Phys.* **2011**, *13*, 19856–19864.
- (32) Bagherzadeh, S. A.; Englezos, P.; Alai, S.; Ripmeester, J. A. Molecular Modeling of the Dissociation of Methane Hydrate in Contact with a Silica Surface. *J. Phys. Chem. B* **2012**, *116*, 3188–3197.
- (33) Chakraborty, S. N.; Gelb, L. D. A Monte Carlo Simulation Study of Methane Clathrate Hydrates Confined in Slit-Shaped Pores. *J. Phys. Chem. B* **2012**, *116*, 2183–2197.
- (34) Hachikubo, A.; Takeya, S.; Chuvilin, E.; Istomin, V. Preservation Phenomena of Methane Hydrate in Pore Spaces. *Phys. Chem. Chem. Phys.* **2011**, *13*, 17449–17452.
- (35) Izumi, F.; Momma, K. Three-Dimensional Visualization in Powder Diffraction. *Solid State Phenom.* **2007**, *130*, 15–20.
- (36) Hirai, H.; Kondo, T.; Hasegawa, M.; Yagi, T.; Yamamoto, Y.; Komai, T.; Nagashima, K.; Sakashita, M.; Fujihisa, H.; Aoki, K. Methane Hydrate Behavior under High Pressure. *J. Phys. Chem. B* **2000**, *104*, 1429–1433.
- (37) Kida, M.; Suzuki, K.; Kawamura, T.; Oyama, H.; Nagao, J.; Ebinuma, T.; Narita, H.; Suzuki, H.; Sakagami, H.; Takahashi, N. Characteristics of Natural Gas Hydrates Occurring in Pore-Spaces of Marine Sediments Collected from the Eastern Nankai Trough, off Japan. *Energy Fuels* **2009**, *23*, 5580–5586.
- (38) Yeon, S. H.; Seol, J.; Seo, Y. J.; Park, Y.; Koh, D. Y.; Park, K. P.; Huh, D. G.; Lee, J.; Lee, H. Effect of Interlayer Ions on Methane Hydrate Formation in Clay Sediments. *J. Phys. Chem. B* **2009**, *113*, 1245–1248.
- (39) Morishige, K.; Uematsu, H. The Proper Structure of Cubic Ice Confined in Mesopores. *J. Chem. Phys.* **2005**, *122*, 044711.
- (40) Smirnov, P.; Yamaguchi, T.; Kittaka, S.; Takahara, S.; Kuroda, Y. X-ray Diffraction Study of Water Confined in Mesoporous MCM-41 Materials over a Temperature Range of 223–298 K. *J. Phys. Chem. B* **2000**, *104*, 5498–5504.
- (41) Yamaguchi, T.; Hashi, H.; Kittaka, S. X-ray Diffraction Study of Water Confined in Activated Carbon Pores over a Temperature Range of 228–298 K. *J. Mol. Liq.* **2006**, *129*, 57–62.
- (42) Muraoka, M.; Nagashima, K. Pattern Variety of Tetrahydrofuran Clathrate Hydrates Formed in Porous Media. *J. Phys. Chem. C* **2012**, *116*, 23342–23350.
- (43) Peppin, S. S. L.; Worster, M. G.; Wettlaufer, J. S. Morphological Instability in Freezing Colloidal Suspensions. *Proc. R. Soc. A* **2007**, *463*, 723–733.
- (44) Seo, Y. T.; Moudrakovski, I.; Ripmeester, J. A.; Lee, J. W.; Lee, H. Efficient Recovery of CO₂ from Flue Gas by Clathrate Hydrate Formation in Porous Silica Gels. *Environ. Sci. Technol.* **2005**, *39*, 2315–2319.
- (45) Takeya, S.; Kida, M.; Minami, H.; Sakagami, H.; Hachikubo, A.; Takahashi, N.; Shoji, H.; Soloviev, V.; Wallmann, K.; Biebow, N.; Obzhairov, A.; Salomatin, A.; Poort, J. Structure and Thermal Expansion of Natural Gas Clathrate Hydrates. *Chem. Eng. Sci.* **2006**, *61*, 2670–2674.